Three-dimensional nanoscale subsurface optical imaging of silicon circuits

E. Ramsay,[a] K. A. Serrels, M. J. Thomson, A. J. Waddie, M. R. Taghizadeh, R. J. Warburton, and D. T. Reid
School of Engineering and Physical Sciences, Heriot-Watt University, Edinburgh EH14 4AS, United Kingdom

(Received 13 September 2006; accepted 20 February 2007; published online 26 March 2007)

Three-dimensional subsurface imaging through the back side of a silicon flip chip is reported with a diffraction-limited lateral resolution of 166 nm and an axial performance capable of resolving features only 100 nm deep. This performance was achieved by implementing sample-scanned two-photon optical beam induced current microscopy using a silicon solid immersion lens and a peak detection algorithm. The excitation source was a 1530 nm erbium:fiber laser, and the lateral optical resolution obtained corresponds to 11% of the free-space wavelength. © *2007 American Institute of Physics*. [DOI: 10.1063/1.2716344]

Sub-100-nm feature sizes are now routine in silicon integrated circuits, and consequently the industry has identified a need for nondestructive wafer/mask level microscopy for measuring the critical dimensions of three-dimensional (3D) structures for defect detection and for general on-chip navigation purposes.[1] In an attempt to address this need using optical imaging, the resolution of subsurface silicon laser-scanning microscopy can be enhanced by the use of a Weierstrass solid immersion lens, also known as a supersolid immersion lens (SSIL), in the back side imaging geometry.[2–5] In this approach an infrared laser is focused through the silicon die, and a silicon SSIL eliminates spherical aberration due to the refractive-index mismatch at the silicon:air interface. Such a SSIL also increases the numerical aperture (NA) of the system—up to a maximum value where the NA equals the refractive index n of the SSIL—and so decreases the focal spot size. Furthermore, during sample-scanned image acquisition, an increase in the spatial sampling frequency also results because of an optical lever effect, where a physical translation of the SSIL and sample results in a proportionately smaller movement of the focused spot. It is well known that in the lateral direction, the reduction factor equals the square of the refractive index, a value of around 12.1 in silicon. In the axial direction, the scaling factor is even greater and suggests the possibility of using high-resolution 3D profiling techniques to visualize the internal morphology of silicon integrated circuits with nanometric resolution.

In silicon devices, standard optical beam induced current microscopy is hindered by the contradictory requirements of choosing a laser wavelength that can penetrate up to several millimeters of silicon but be absorbed sufficiently in the micron-scale device layer to produce high contrast images. The issue of penetration is also encountered in conventional confocal imaging using light at 1064 nm, where the proximity of the band edge means that the absorption coefficient is around 80 cm^{-1} and the light must be double passed through the silicon. In both cases the introduction of a SSIL causes further absorption. An elegant solution is to use the two-photon optical beam induced current (TOBIC) effect[6] to achieve high absorption of infrared radiation at the beam focus but high transmission elsewhere in the sample and in the SSIL. Using two-photon absorption, the lateral resolution of the microscope is improved, and the ability to implement axially-resolved imaging is provided because two-photon absorption is highly dependent on the optical intensity. In this letter we report two-dimensional (2D) diffraction-limited imaging performance with a resolution of 166 nm and an extension to 3D subsurface imaging with approximately 100 nm axial profiling resolution. This result improves on earlier performance obtained using a similar system,[7] and we attribute it to a better ability to perform systematic axial scanning and thus localize the focus of the beam in the component layer of the chip more accurately.

We used a 1530 nm mode locked erbium-fiber laser to provide nonlinear excitation, and the experimental arrangement is shown in Fig. 1. The Gaussian laser beam, full width at half maximum diameter of 3.3 mm, overfilled the 3 mm diameter pupil of the objective lens, and using a Gaussian beam decomposition method implemented in ray-tracing software (ASAP, Breault Research Organization) we calculated a focal spot size of 240 nm. We also determined the point spread function (PSF) at 1530 nm using analytic formulas expressed in terms of the system numerical aperture (NA) and valid for high NA.[8] The NA of the imaging system

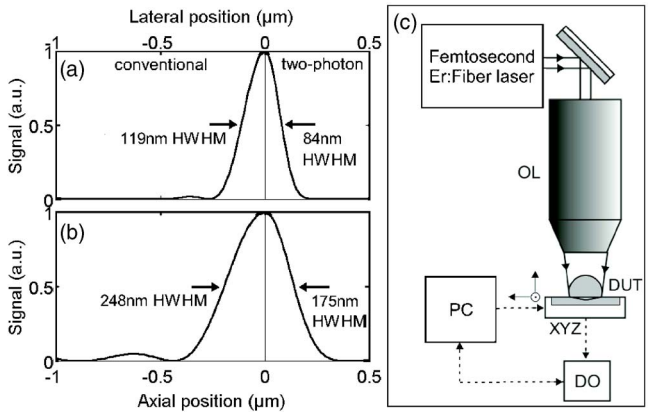

FIG. 1. (a) Lateral and (b) axial point spread functions calculated for beam focused in a silicon sample by a silicon SSIL. (c) Sample-scanning nonlinear microscope: *XYZ*, three-axis motorized scanning stages; DUT, device under test; PC, personal computer; OL, Mitutoyo 20X M Plan Apo NIR NA of 0.42 objective lens, DO, digital oscilloscope.

[a]Electronic mail: e.ramsay@hw.ac.uk

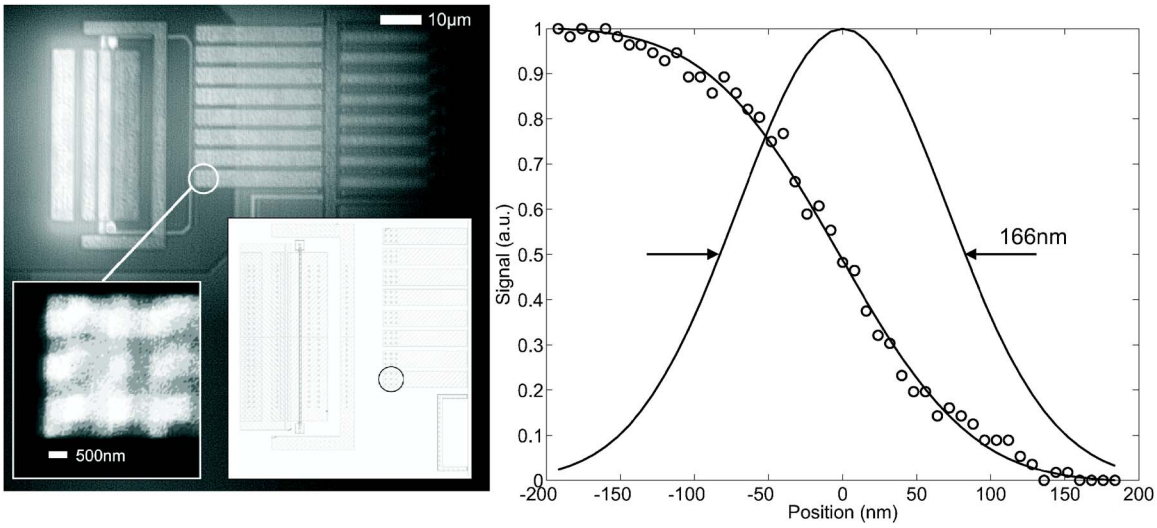

FIG. 2. (a) Medium resolution TOBIC image of the device showing (right inset) a design schematic of the same area, and (left inset) a high-resolution TOBIC image of the matrix of contacts at the end of a metal finger. (b) Lateral resolution measurement across the edge of one finger showing 166 nm resolution. The solid fitting line is the integral of the Gaussian point spread function shown in the figure.

is limited only by the maximum ray angle reaching the sample and by the refractive index of the immersion material. The refractive index of silicon at 1530 nm is 3.48,[9] and a simple ray-tracing analysis implied a maximum usable NA of 3.4. For this NA value, the PSFs calculated for the overfilled pupil are shown in Figs. 1(a) and 1(b) and have diameters of 238 nm (lateral) and 496 nm (axial). Taking account of the $\sqrt{2}$ reduction in resolution caused by nonlinear imaging, the PSF diameters become 168 nm (lateral) and 350 nm (axial). The laser generated 400 fs pulses at a repetition frequency of 30 MHz with an average output power of 75 mW, and its output was focused by an objective lens of NA of 0.42 through a SSIL into the device under test [see Fig. 1(c)]. The sample was a 350 nm feature size flip chip with an exposed substrate of 100 μm thickness. Our SSIL was designed using the standard prescription for obtaining the maximum NA, which states that to image a structure buried at a depth X below the surface requires a SSIL whose vertical thickness D is given by $D=R(1+1/n)-X$ where R is the lens radius of curvature.[2] A photo-voltage of up to 200 mV was generated through two-photon carrier generation at the device layer of the chip, and this signal was detected using a digital oscilloscope and recorded on a desktop personal computer (PC). The PC also controlled the motorized three-axis translation stages on which the device was situated and which had a physical stepping increment of 100 nm at a velocity of 156 steps/s. Higher velocities caused the SIL to slip on the surface of the chip, but this can be solved by using beam-scanned imaging which is compatible with SIL microscopy and provides faster image acquisition. At the low pixel acquisition rates used here, we were able to reduce the noise by narrow-band amplification or lock-in detection, and both techniques were used in acquiring the data presented here.

The main section of Fig. 2(a) shows an image acquired using coarse stepping (10 μm physical; 800 nm optical) to provide a map suitable for navigation purposes. Previous work used the same sample to confirm the 12.1 scaling factor relating the physical displacement of the sample to the movement of the focal spot.[7] The lateral resolution was evaluated by recording a higher resolution image of the area [left inset, Fig. 2(a)]. This region contained an area of n-doped silicon under metal, and a resolution measurement of 166 nm was inferred from a line scan taken across the edge of this feature, which can be seen in Fig. 2(b). The solid fitting line shown in Fig. 2(b) is the integral of the Gaussian point spread function also shown in the same figure. At this resolution we were able to clearly resolve individual features which we believe from design information are tungsten contacts or vias arranged in a 3×3 grid at separations of 1.25 μm. The right inset of Fig. 2(a) shows these contacts on the design schematic for the device (circled). The experimental resolution of 166 nm essentially matches the calculated value (168 nm) to within the limits of experimental precision. Our system is therefore diffraction limited in the lateral direction with a resolution corresponding to just 11% of the free-space wavelength.

The strength of the TOBIC signal is sensitive to the axial position of the beam focus relative to any feature in the device, therefore a peak detection procedure can be used to profile the 3D morphology of subsurface features. Unlike lateral motion, the subsurface focal spot movement caused by axially translating the sample is not simple to analyze analytically. Using ASAP ray-tracing software, we modeled the movement of the position of the smallest focused spot against the physical movement of the SSIL, the gradient of which gives the physical/optical scaling factor. The logarithm of this scaling factor was then plotted against the logarithm of the refractive index of the simulated SSIL. In the literature[2] the axial scaling factor of a SSIL is stated as n^3. The results of our model show a nonuniform scaling factor in n, although for our particular refractive index the scaling factor is calculated to be $\sim$75, whereas n^3 would imply a factor of 42. The behavior of a hemispherical solid immersion lens (HSIL) in the axial direction shows a scaling factor of n, although for high refractive indices, even this ceases to be exact. The difference between our axial scaling factor and that quoted in the literature for a SSIL is due to the fact that the n^3 factor only applies to paraxial rays.[10] In our model, we assume that the light is focused at the point where the bundle of rays propagating through the system has the smallest width, which leads to a nonuniform scaling factor. This

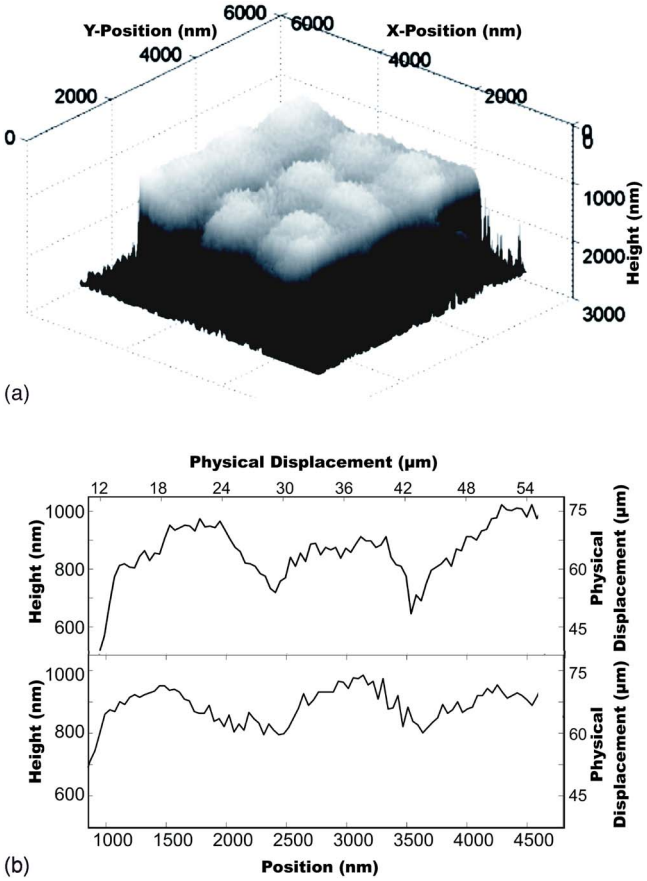

FIG. 3. (a) TOBIC height profile of the matrix of contacts shown in Fig. 2. The physical separation between the contacts is 1.25 μm. (b) Cross sections of the central three contacts taken in the *X* and *Y* directions.

method was chosen because the smallest spot size is where the most efficient two-photon absorption occurs. In our simulations, a factor of $n^3 \sim 42$ was obtained by propagating only the paraxial rays in the system and looking for the point where those rays cross the optical axis of the objective lens, whereas a factor of 161 was obtained by propagating only the extreme rays.

3D profiling was performed by acquiring a set of 2D images, each one recorded at a different axial position of the sample. In the resulting data cube, a peak detection algorithm was used to find the axial position corresponding to the maximum TOBIC signal at each lateral position in the XY plane.[11] We concentrated 3D profiling on the area of the device containing the 3×3 grid of contacts with the aim of determining their height. Figure 3(a) shows a 3D profile of the area, and Fig. 3(b) shows cross sections through this image. The height scale was calibrated using the results of the ray-tracing model described earlier. The results indicate that the contacts have a height of ~160 nm, based on the difference in the maximum photocurrent measured when the beam is focused either on or between the contacts. The absolute contact height, as inferred from the cross-sectional data [Fig. 3(b)], is consistent to ±60 nm. The axial PSF calculations presented in Fig. 1(b) indicate an optimal resolution of 350 nm under nonlinear imaging, and experimentally we show approximate profiling resolutions of ~100 nm. This resolution appears to exceed the diffraction-limited performance; however, it is well known that peak detection strategies can allow features much smaller than the axial resolution to be profiled.[12]

In summary, we have demonstrated imaging of subsurface features in 3D with lateral resolutions of 166 nm and axial resolutions capable of resolving individual nanoscale features with heights of around 100 nm. We anticipate further improvements by implementing TOBIC at shorter excitation wavelengths and by using other resolution enhancing techniques to manipulate the point spread function.

The authors gratefully acknowledge financial support from the UK Engineering and Physical Sciences Research Council under Grant No. EP/C509765/1. One of the authors (K.A.S.) acknowledges financial support from the UK Engineering and Physical Sciences Research Council under a Doctoral Training Award. The support of Credence Inc. is also gratefully acknowledged.

[1] International Technology Roadmap for Semiconductors (2003).
[2] S. B. Ippolito, B. B. Goldberg, and M. S. Unlu, Appl. Phys. Lett. **78**, 4071 (2001).
[3] Q. Wu, G. D. Feke, R. D. Grober, and L. P. Ghislain, Appl. Phys. Lett. **75**, 4064 (1999).
[4] Q. Wu, L. P. Ghislain, and V. B. Elings, Proc. IEEE **88**, 1491 (2000).
[5] O. Breitenstein, F. Altmann, T. Riediger, D. Karg, and V. Gottschalk, Microelectron. Reliab. **46**, 1508 (2006).
[6] C. Xu and W. Denk, Appl. Phys. Lett. **71**, 2578 (1997).
[7] E. Ramsay, N. Pleynet, D. Xiao, R. J. Warburton, and D. T. Reid, Opt. Lett. **30**, 26 (2005).
[8] T. Wilson, *Confocal Microscopy* (Academic, London, 1990).
[9] Silicon refractive index is from Crystran U.K. Ltd.
[10] M. S. Unlu, M. G. Eraslan, Z. Liu, A. N. Vamivakas, S. A. Thorne, S. B. Ippolito, and B. B. Goldberg, Abstr. Pap. - Am. Chem. Soc. **227**, U250 (2004).
[11] E. Ramsay, D. T. Reid, and K. Wilsher, Appl. Phys. Lett. **81**, 7 (2002).
[12] C. J. R. Sheppard and D. M. Shotton, *Confocal Laser Scanning Microscopy* (Bios Scientific, Oxford, 1997).